Electronic Supplementary Information

The Construction of AIE-Based Controllable Singlet Oxygen Generation System Directed by Supramolecular Strategy

Weirui Qian,[a] Minzan Zuo,[a] Guangping Sun,[a] Yuan Chen,[a] Tingting Han,[a] Xiao-Yu Hu,*[b] Ruibing Wang,[c] and Leyong Wang*[a]

[a] *Key Laboratory of Mesoscopic Chemistry of MOE, Jiangsu Key Laboratory of Advanced Organic Materials, School of Chemistry and Chemical Engineering, Nanjing University, Nanjing, 210023, China. E-mail: lywang@nju.edu.cn (LW).*

[b] *Applied Chemistry Department, School of Material Science and Engineering, Nanjing University of Aeronautics and Astronautics, Nanjing, 211100, China. E-mail: huxy@nuaa.edu.cn (XH).*

[c] *State Key Laboratory of Quality Research in Chinese Medicine, Institute of Chinese Medical Sciences, University of Macau, Taipa, Macau, China.*

Table of Contents

1. General information and experimental procedures

1.1 General information

All reactions were performed in air atmosphere unless otherwise stated. Reagents were commercially available and used without further purification. Column chromatography was performed with silica gel (200−300 mesh) produced by Qingdao Marine Chemical Factory, Qingdao (China). All yields were given as isolated yields. NMR spectra were recorded on a Bruker DPX 400 MHz spectrometer with internal standard tetramethylsilane (TMS) and solvent signals as internal references at 298 K. The chemical shifts (δ) were expressed in ppm and J values were given in Hz. High-resolution electrospray ionization mass spectra (HR-ESI-MS) were recorded on an Agilent 6540Q-TOF LCMS equipped with an electrospray ionization (ESI) probe. The UV−Vis absorption spectra were measured on a Perkin Elmer Lambda 35 UV−Vis Spectrometer. The ITC experiment was performed on an ITC 200 micro-calorimeter (GE Company, USA). Dynamic light scattering (DLS) measurements were carried out on a Brookhaven BI-9000AT system (Brookhaven Instruments Corporation, USA), using a 200 mW polarized laser source (λ = 514 nm). Transmission electron microscope (TEM) investigations were carried out on a JEM−2100 instrument. The excitation and emission spectra were recorded on a Hitachi F−7000 Fluorescence Spectrometer. The deionized water was prepared by a Millipore NanoPure purification system.

1.2 Experimental procedures

Fabrication of the WP5⊃TPEPY supramolecular nanoparticles. WP5⊃TPEPY nanoparticles were prepared as follows: The stock solution of **TPEPY** (5.0 mM, dissolved in MeOH) and **WP5** (1.0 mM, dissolved in water) were prepared. Then, 75 μL of **WP5** solution was added into a volumetric flask (5 mL) and 4.92 mL of water was added to dilute **WP5** solution. Finally, 15 μL of **TPEPY** was quickly injected into the above solution to generate the nanoparticle solutions. The ultimate concentrations of **WP5** and **TPEPY** were 15 μM and 15 μM, respectively.

2. Synthesis of guest molecule TPEPY

The synthetic procedures of guest molecule **TPEPY** were shown in **Scheme S1**

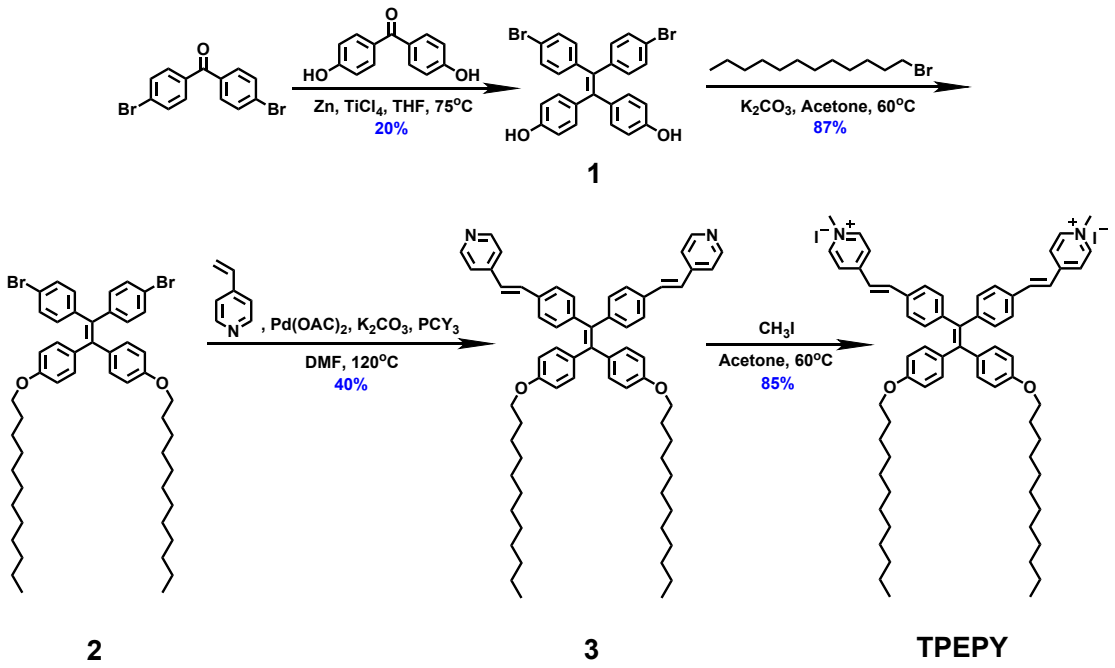

Scheme S1 Synthetic route of guest molecule **TPEPY**.

2.1 Synthesis of compound 1

Compound **1** was prepared according to reported literature.[S1]

To a mixture of 4,4′-dibromobenzophenone (1.7 g, 5.0 mmol), 4,4′-dihydroxybenzophenone (1.1 g, 5.0 mmol) and zinc dust (6.5 g, 0.10 mol) in dry THF (60 mL), titanium (IV) chloride (3.8 g, 20 mmol) was added slowly under argon atmosphere at −78 °C. After stirring for 20 min, the reaction mixture was warmed to room temperature and then heated to reflux for 12 h. Potassium carbonate solution (10 %, 80 mL) was added to quench the reaction at room temperature and the mixture was extracted with dichloromethane (DCM) by three times. The combined organic layers were dried over Na_2SO_4, filtered, and concentrated. The crude product was purified by silica gel chromatography using petroleum ether (PE)/ethyl acetate (EA) (8:1, *v/v*) as the eluent to afford compound **1** as a white solid (0.52 g, 1.0 mmol, 20 %). ^{1}H NMR (400 MHz, DMSO-d_6, 298 K) δ (ppm): 9.42 (s, 2H), 7.34 (d, J = 8.4 Hz, 4H), 6.87 (d, J = 8.8 Hz, 4H), 6.75 (d, J = 8.8 Hz, 4H), 6.54 (d, J = 8.4 Hz, 4H).

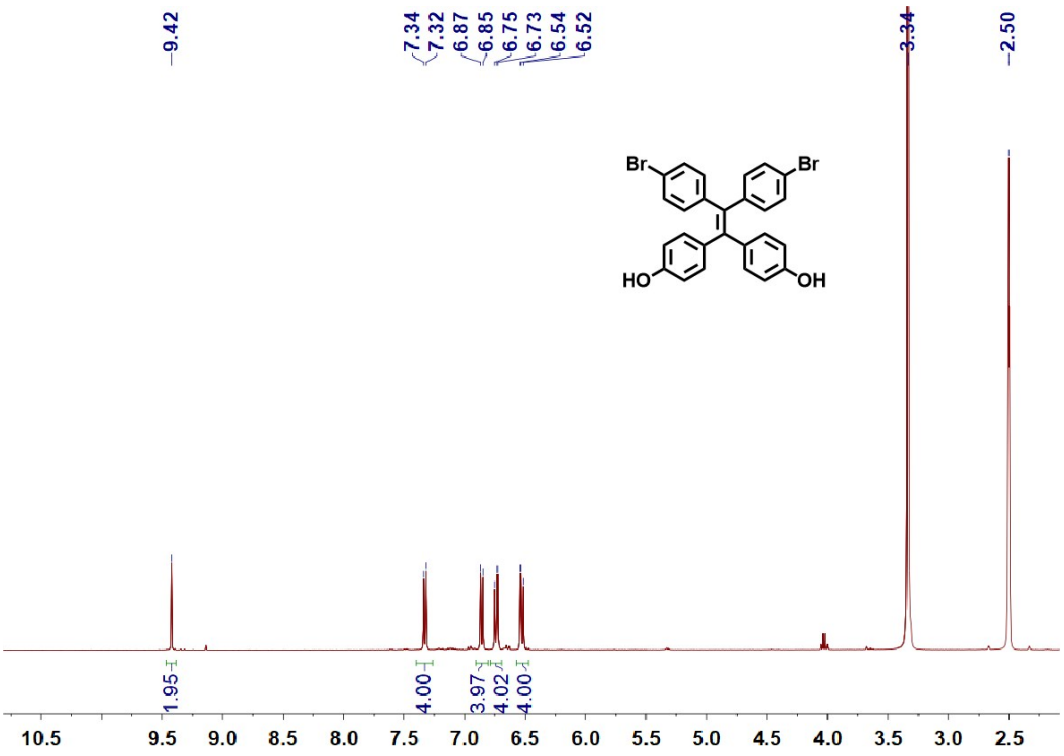

Fig. S1 ^{1}H NMR spectrum of compound **1** (400 MHz, DMSO-d_6, 298 K).

2.2 Synthesis of compound 2

Compound **2** was prepared according to reported literature.[S2]

To a solution of compound **1** (0.42 g, 0.80 mmol) in acetone (25 mL), 1-bromododecane (0.99 g, 4.0 mmol) and potassium carbonate (0.66 g, 4.80 mmol) were added and the mixture was refluxed for 12 h. After removal of the solvent under reduced pressure, the crude product was purified by silica gel chromatography using petroleum ether (PE)/dichloromethane (DCM) (10:1, *v/v*) as the eluent to afford compound **2** as a pale yellow clear oil (0.60 g, 0.70 mmol, 87 %). ^{1}H NMR (400 MHz, $CDCl_3$, 298 K) δ (ppm): 7.23 (d, J = 8.4 Hz, 4H), 6.85−6.89 (m, 8H), 6.64 (d, J = 8.8 Hz, 4H), 3.88 (t, J = 6.4 Hz, 4H), 1.71−1.78 (m, 4H), 1.39−1.43 (m, 4H), 1.26−1.30 (m, 32H), 0.86−0.90 (m, 6H). ^{13}C NMR (100 MHz, $CDCl_3$, 298 K) δ (ppm): 158.0, 142.9, 141.7, 136.3, 135.4, 133.0, 132.5, 131.0, 120.2, 113.7, 67.9, 31.9, 29.7, 29.6, 29.6, 29.6, 29.4, 29.4, 29.3, 26.1, 22.7, 14.1.

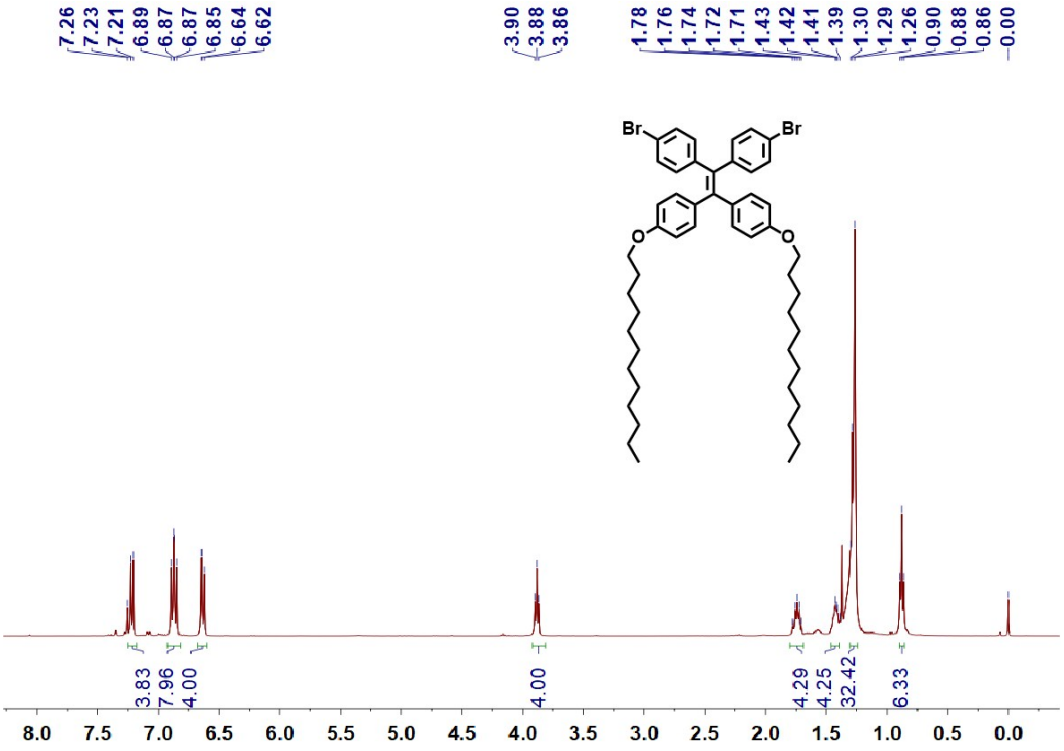

Fig. S2 ^{1}H NMR spectrum of compound **2** (400 MHz, $CDCl_3$, 298 K).

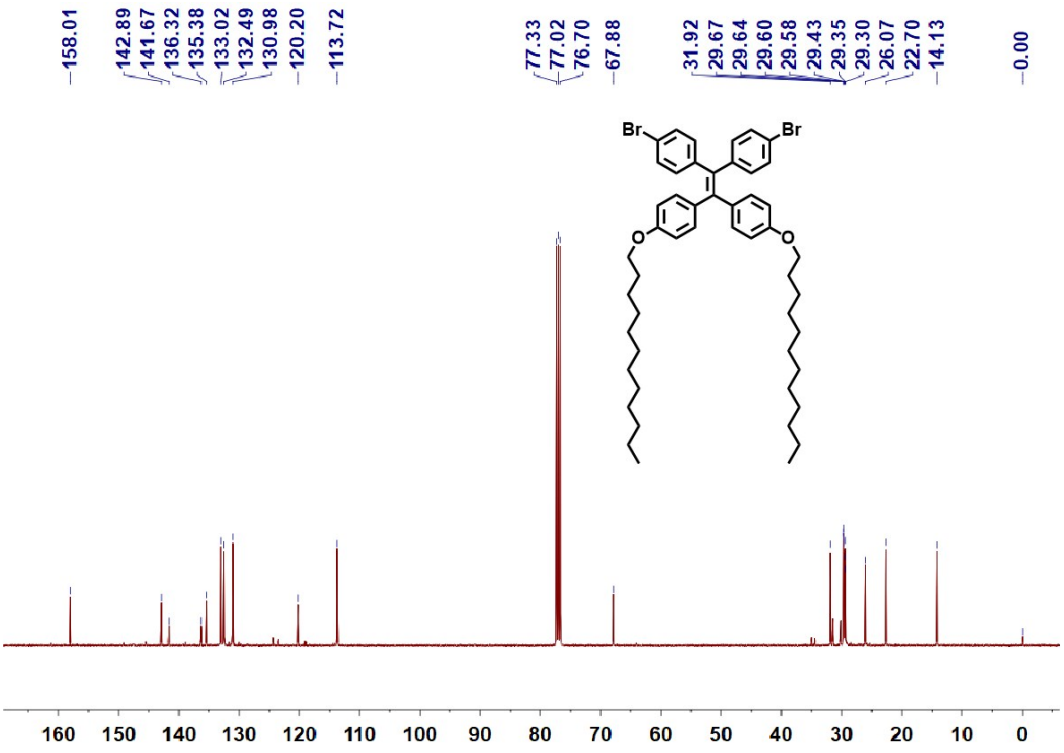

Fig. S3 ^{13}C NMR spectrum of compound **2** (100 MHz, $CDCl_3$, 298 K).

2.3 Synthesis of compound 3

To a solution of compound **2** (0.26 g, 0.30 mmol) in dry DMF (15 mL), potassium carbonate (0.33 g, 2.4 mmol) was added. After degassing, $Pd(OAC)_2$ (0.090 g, 0.38 mmol), PCY_3 (0.090 g, 0.33 mmol) and 4-vinyl pyridine (0.19 g, 1.8 mmol) were added and the resulting mixture was heated to 110 °C for 48 h. After removal of the solvent under reduced pressure, the crude product was purified by silica gel chromatography using petroleum ether (PE)/ethyl acetate (EA) (1:1, *v/v*) as the eluent to afford compound **3** as a bright yellow solid (0.11 g, 0.12 mmol, 40 %). ^{1}H NMR (400 MHz, $CDCl_3$, 298 K) δ (ppm): 8.56 (d, J = 6.4 Hz, 4H), 7.36 (d, J = 6.4 Hz, 4H), 7.31 (d, J = 8.4 Hz, 4H), 7.25 (d, J = 16.4 Hz, 2H), 7.06 (d, J = 8.4 Hz, 4H), 6.92−6.96 (m, 6H), 6.65 (d, J = 8.8 Hz, 4H), 3.88 (t, J = 6.4 Hz, 4H), 1.70−1.77 (m, 4H), 1.40−1.47 (m, 4H), 1.26−1.33 (m, 32H), 0.86−0.89 (m, 6H). ^{13}C NMR (100 MHz, $CDCl_3$, 298 K) δ (ppm): 158.0, 149.6, 145.3, 145.1, 141.8, 137.6, 135.8, 133.8, 133.4, 132.7, 132.0, 126.6, 125.3, 120.9, 113.7, 67.90, 31.9, 29.7, 29.6, 29.6, 29.6, 29.4, 29.3, 29.3, 26.1, 22.7, 14.1. HR-ESI-MS: m/z calcd $[M+H]^+$ 907.6136, found 907.6138.

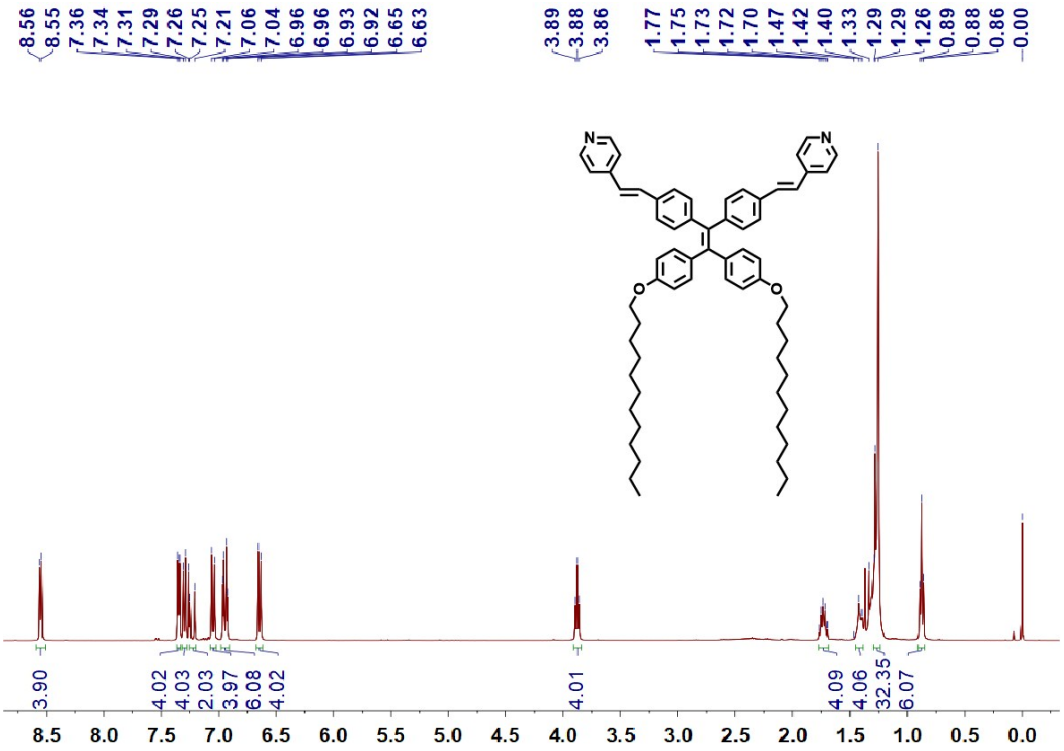

Fig. S4 ^{1}H NMR spectrum of compound **3** (400 MHz, $CDCl_3$, 298 K).

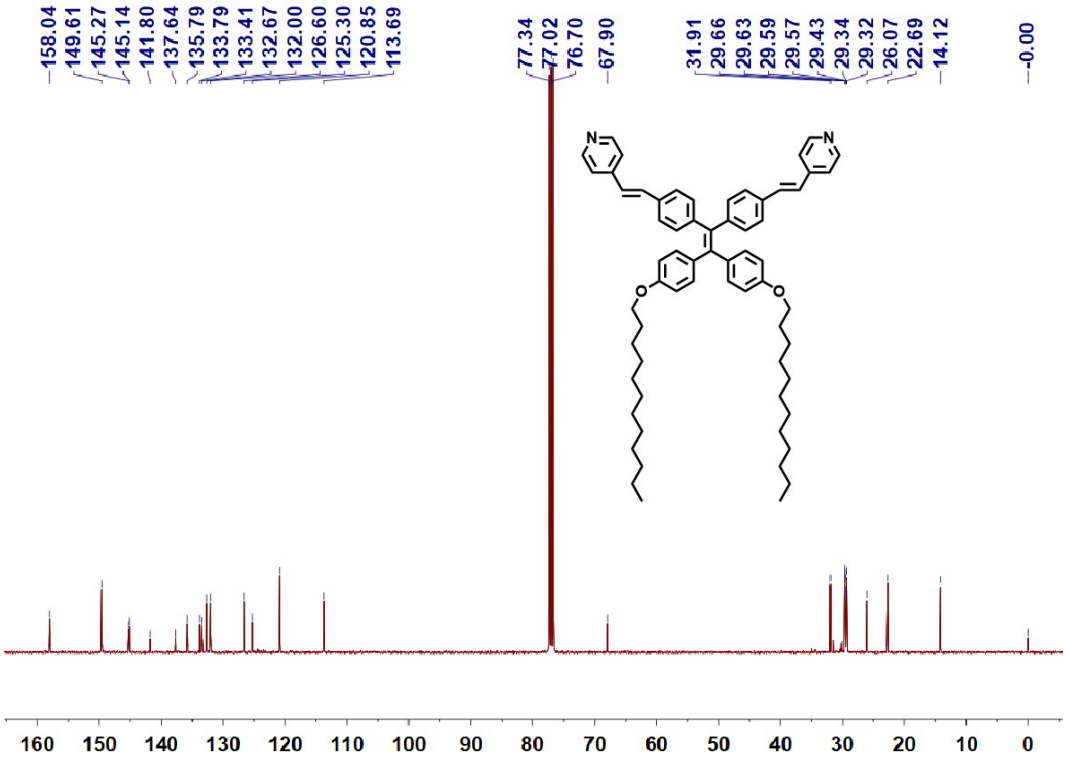

Fig. S5 ^{13}C NMR spectrum of compound **3** (100 MHz, $CDCl_3$, 298 K).

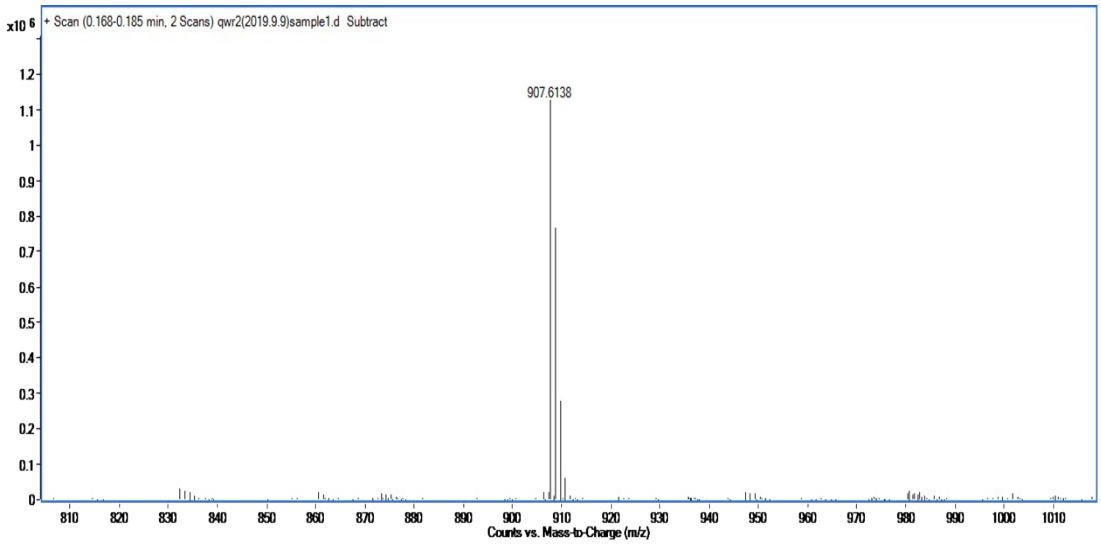

Fig. S6 HR-ESI-MS spectrum of compound **3**.

2.4 Synthesis of compound TPEPY

To a solution of compound **3** (0.11 g, 0.12 mmol) in acetone (25 mL), iodomethane (1.0 g, 7.2 mmol) was added and the solution was refluxed for 24 h. The solvent was removed under vacuum and the crude product was washed several times by PE to afford compound **TPEPY** as a red solid (0.12 g, 0.10 mmol, 85 %). ^{1}H NMR (400 MHz, DMSO-d_6, 298 K) δ (ppm): 8.84 (d, J = 6.4 Hz, 4H), 8.17 (d, J = 6.4 Hz, 4H), 7.93 (d, J = 16.4 Hz, 2H), 7.56 (d, J = 8.0 Hz, 4H), 7.46 (d, J = 16.4 Hz, 2H), 7.08 (d, J =

8.0 Hz, 4H), 6.91 (d, J = 8.4 Hz, 4H), 6.72 (d, J = 8.4 Hz, 4H), 4.25 (s, 6H), 3.87 (t, J = 6.0 Hz, 4H), 1.63−1.67 (m, 4H), 1.23−1.36 (m, 32H), 0.85 (m, 6H).^{13}C NMR (100 MHz, DMSO-d_6, 298 K) δ (ppm): 158.1, 152.9, 146.4, 145.6, 142.7, 140.6, 137.8, 135.6, 133.7, 132.7, 132.1, 128.3, 123.9, 123.6, 114.3, 67.8, 63.3, 47.4, 31.8, 29.5, 29.5, 29.4, 29.3, 29.2, 29.2, 26.0, 22.6, 14.4. HR-ESI-MS: m/z calcd $[M-2I]^{2+}$ 468.3261, found 468.3265.

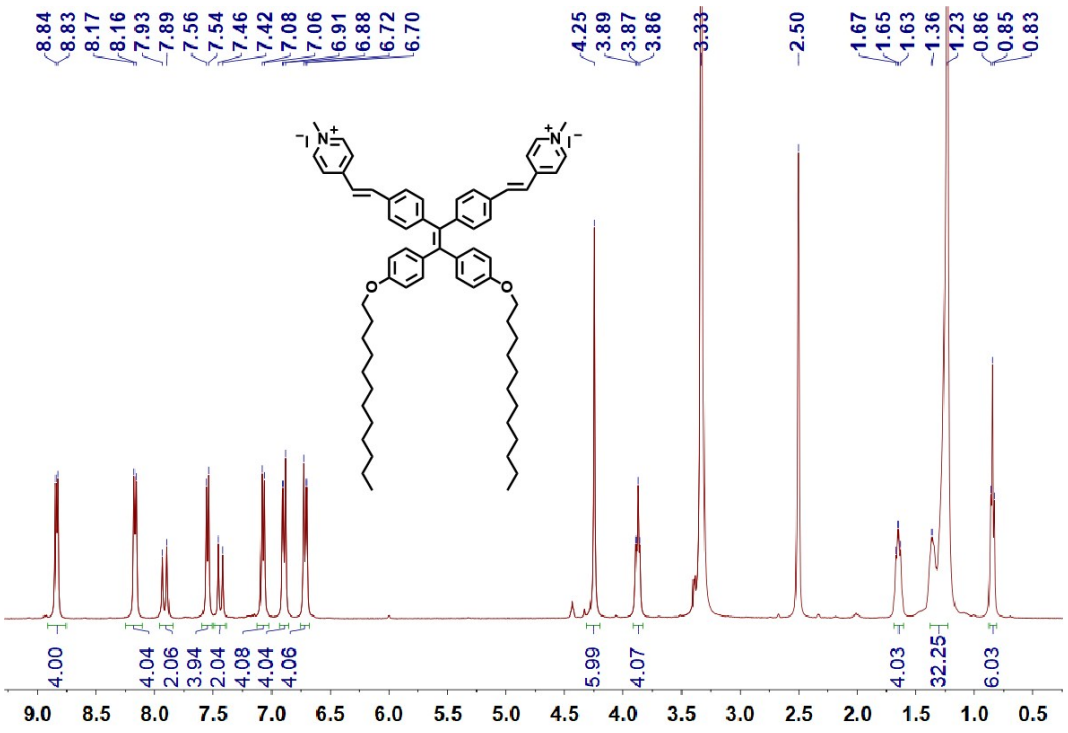

Fig. S7 ^{1}H NMR spectrum of compound **TPEPY** (400 MHz, DMSO-d_6, 298 K).

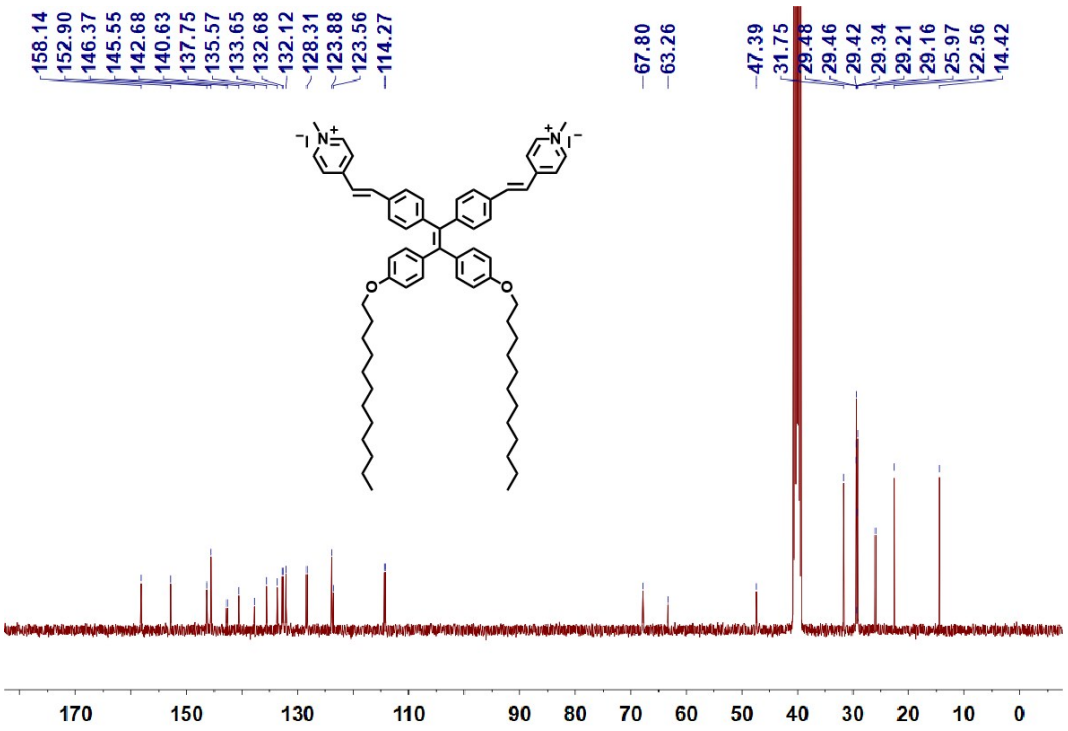

Fig. S8 ^{13}C NMR spectrum of compound **TPEPY** (100 MHz, DMSO-d_6, 298 K).

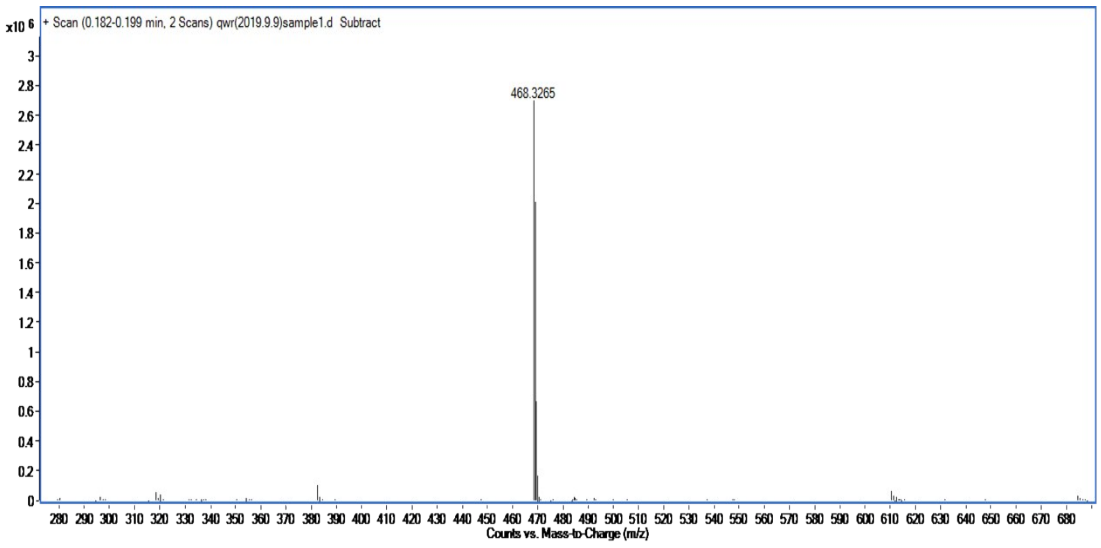

Fig. S9 HR-ESI-MS spectrum of compound **TPEPY**.

3. Binding capacity studies between different macrocyclic molecules and G′

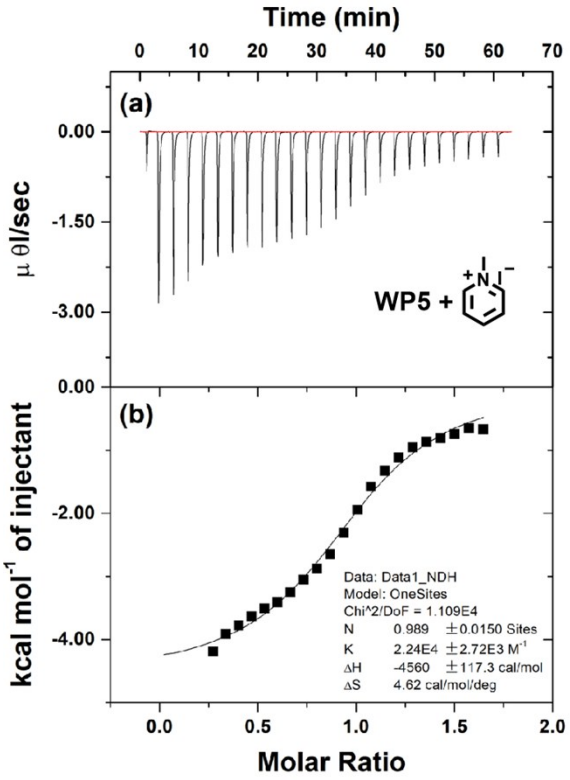

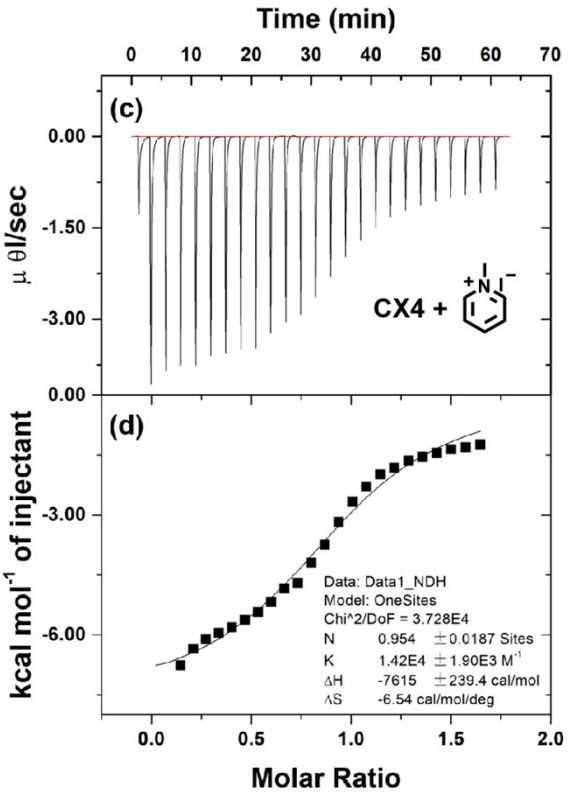

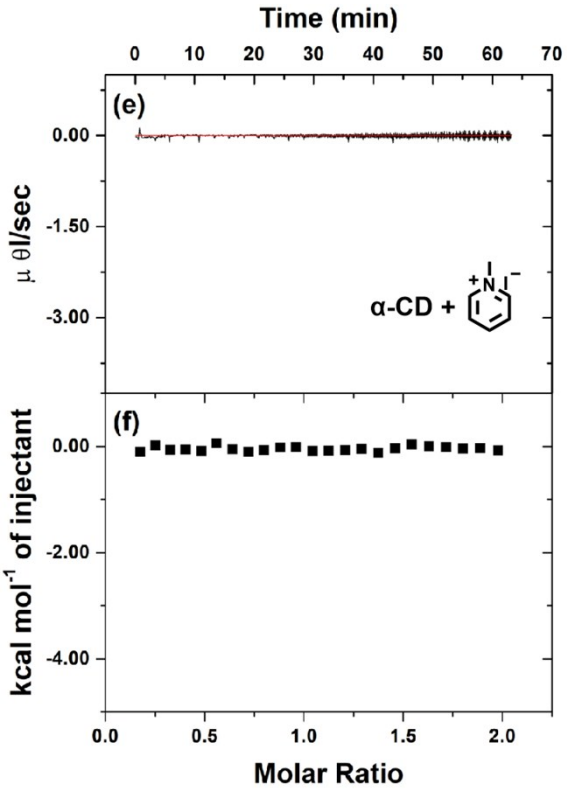

Fig. S10 Microcalorimetric titrations between different macrocyclic molecule and **G′** in water at 298.15 K. Raw ITC data of **G′** ([cell] = 0.6 mM) with different macrocyclic hosts ([syringe] = 5.0 mM): (a) **WP5**, (c) **CX4**, and (e) **α-CD** in water. "S-type" heat effects between **G′** and **WP5** (b), **CX4** (d), and **α-CD** (f) for each injection (obtained by subtracting the dilution heat), and the data were fitted by computer simulation with the "one set of binding sites" model.

4. UV−Vis absorption and photoluminescence spectra of TPEPY

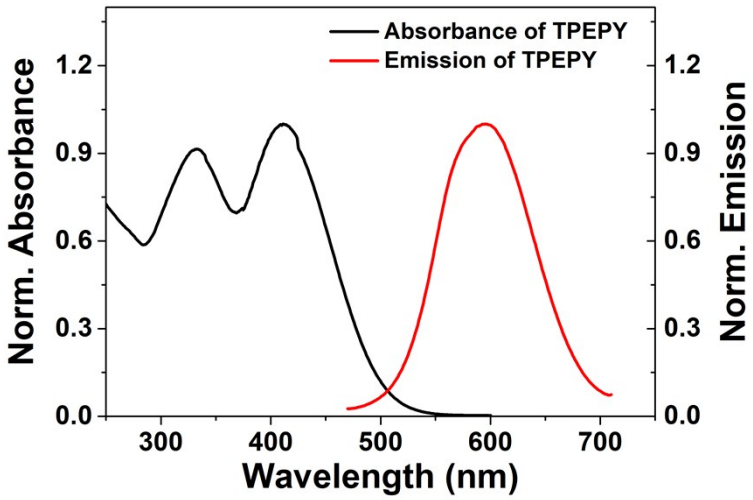

Fig. S11 The UV−Vis absorption and photoluminescence spectra of **TPEPY** (λ_{ex} = 365 nm) in aqueous media. [**TPEPY**] = 15 μM.

5. Absorbance decay of ABDA in the presence of TPEPY with different macrocyclic molecules

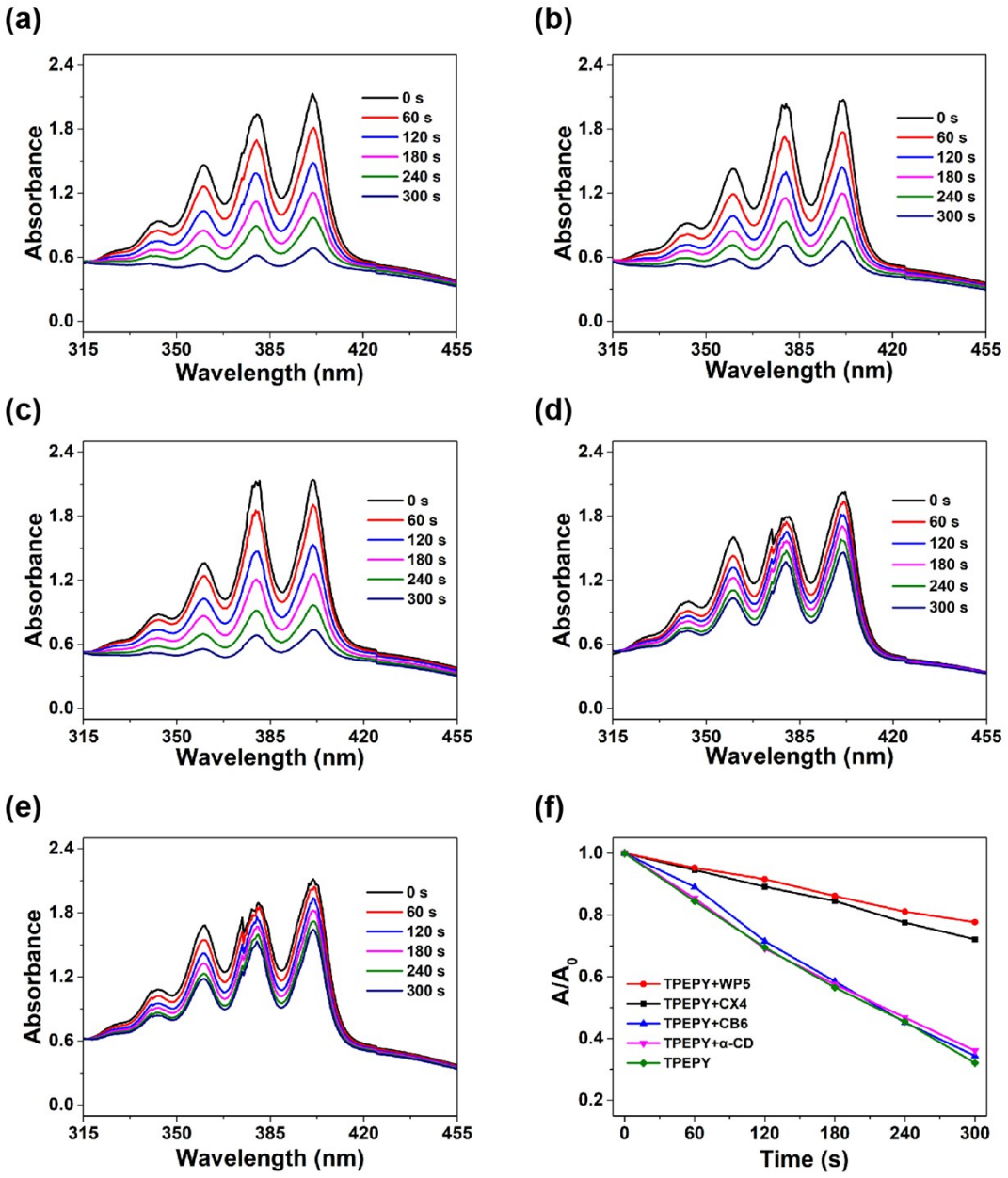

Fig. S12 (a) UV−Vis spectra of 9,10-anthracenediyl-bis(methylene)dimalonic acid (ABDA) in the presence of **TPEPY** under white light irradiation (400−700 nm, 10 mW·cm^{-2}). UV−Vis spectra of ABDA in the presence of **TPEPY** with **α-CD** (b), **CB6** (c), **CX4** (d), and **WP5** (e) under white light irradiation (400−700 nm, 10 mW·cm^{-2}). (f) Normalized degradation percentages of ABDA at 401 nm in the presence of **TPEPY** with different macrocyclic molecules under white light irradiation (400−700 nm, 10 mW·cm^{-2}). [**TPEPY**] = 15 μM, [**α-CD**] = 15 μM, [**CB6**] = 15 μM, [**CX4**] = 15 μM, [**WP5**] = 15 μM, and [ABDA] = 0.20 mM.

6. Absorbance decay of ABDA in the presence of TPEPY with varied concentrations of WP5

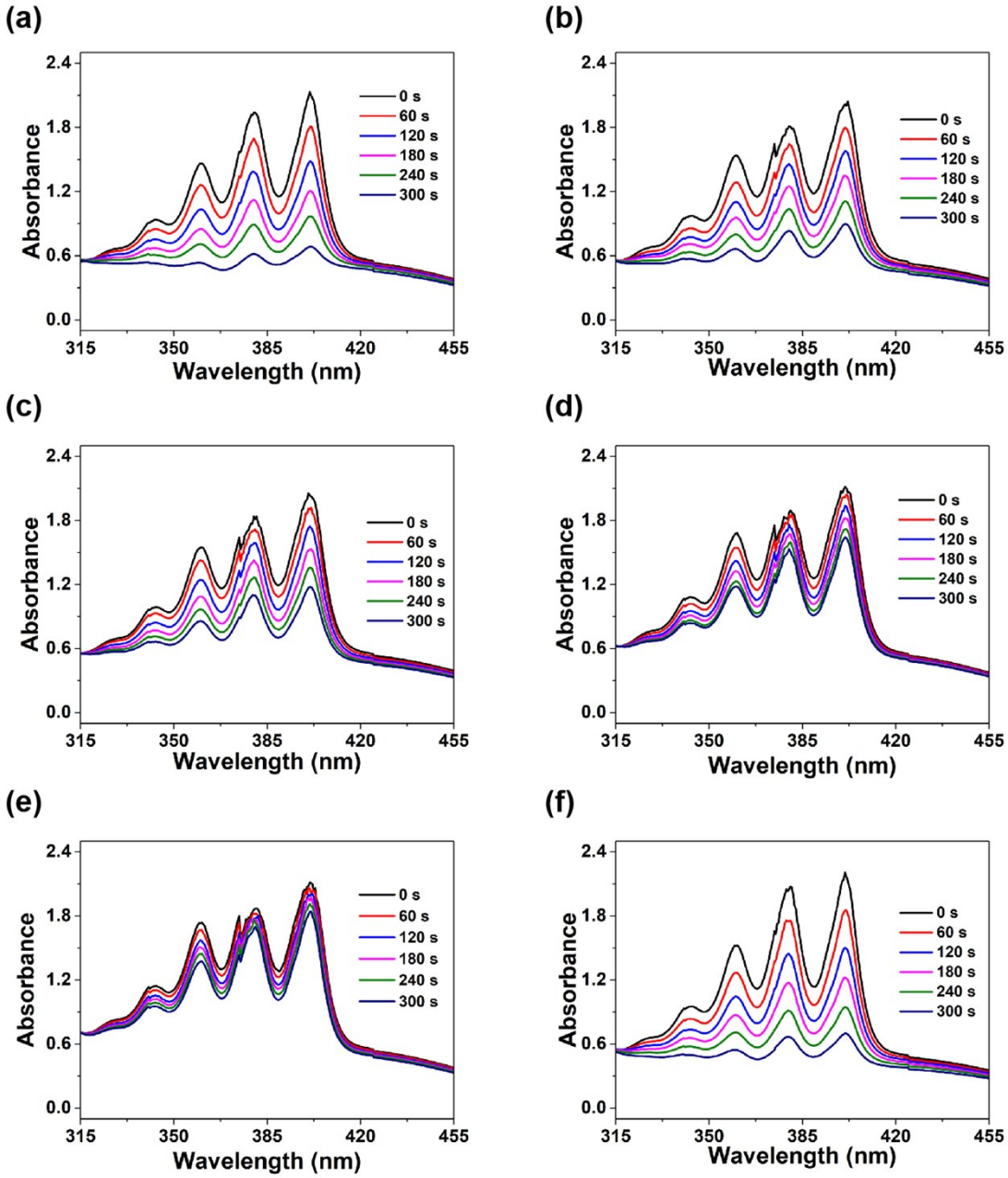

Fig. S13 UV−Vis spectra of ABDA in the presence of **TPEPY** with different concentrations of **WP5**: [**WP5**] = 0 μM (a), [**WP5**] = 0.94 μM (b), [**WP5**] = 3.75 μM (c), [**WP5**] = 15 μM (d), and [**WP5**] = 60 μM (e) under white light irradiation (400−700 nm, 10 mW·cm^{-2}). (f) UV−Vis spectra of ABDA in the presence of **TPEPY** with **M** ([**M**] = 0.37 mM) under white light irradiation (400−700 nm, 10 mW·cm^{-2}). [**TPEPY**] = 15 μM, [ABDA] = 0.20 mM.

7. Absorbance decay of ABDA in the presence of RB with WP5

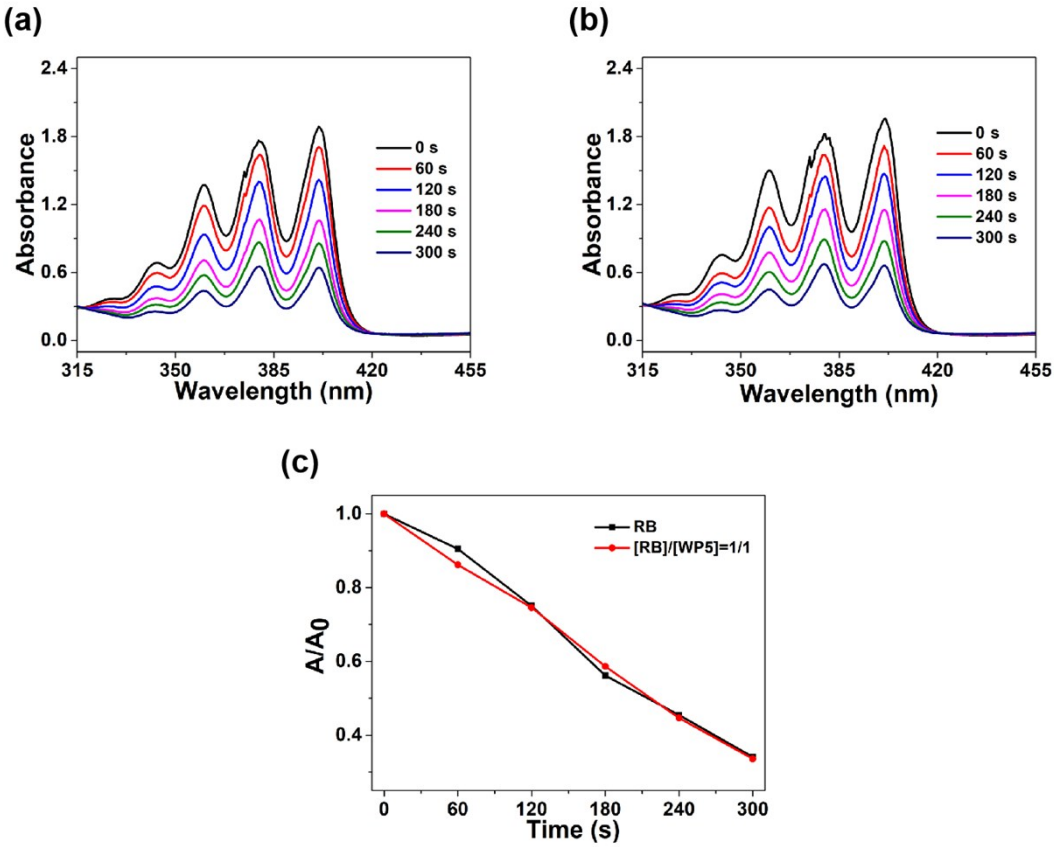

Fig. S14 UV−Vis spectra of ABDA in the presence of Rose Bengal (**RB**) without **WP5** (a), and with **WP5** ([**WP5**] = 15 μM) (b) under white light irradiation (400−700 nm, 10 mW·cm^{-2}). (c) Normalized degradation percentages of ABDA at 401 nm in the presence of **RB** with and without **WP5** under white light irradiation (400−700 nm, 10 mW·cm^{-2}). [**RB**] = 15 μM, [ABDA**]** = 0.20 mM.

8. Tyndall effect of WP5⊃TPEPY nanoassemblies

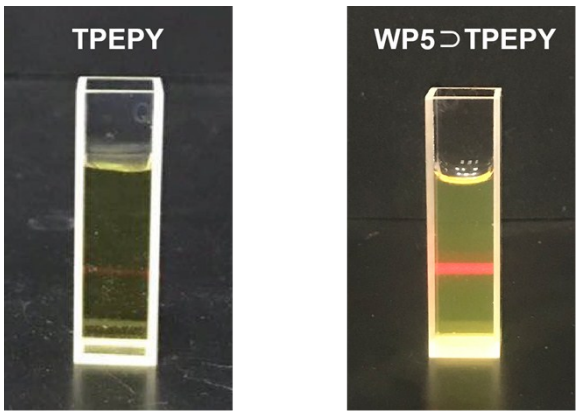

Fig. S15 Tyndall effect of free **TPEPY** solution (25 μM, containing 0.5% methanol) and **WP5⊃TPEPY** solution ([**TPEPY**] = 25 μM, [**WP5**] = 6.25 μM, containing 0.5% methanol).

9. Determination of the best molar ratio between WP5 and TPEPY

As is shown in Fig. S16, upon gradually increasing the concentration of **WP5**, the transmittance at 700 nm first underwent a rapid decrease to a minimum and thereafter an inverse increase. Thus, the best molar ratio for the formation of supramolecular aggregates was observed at the inflection point.

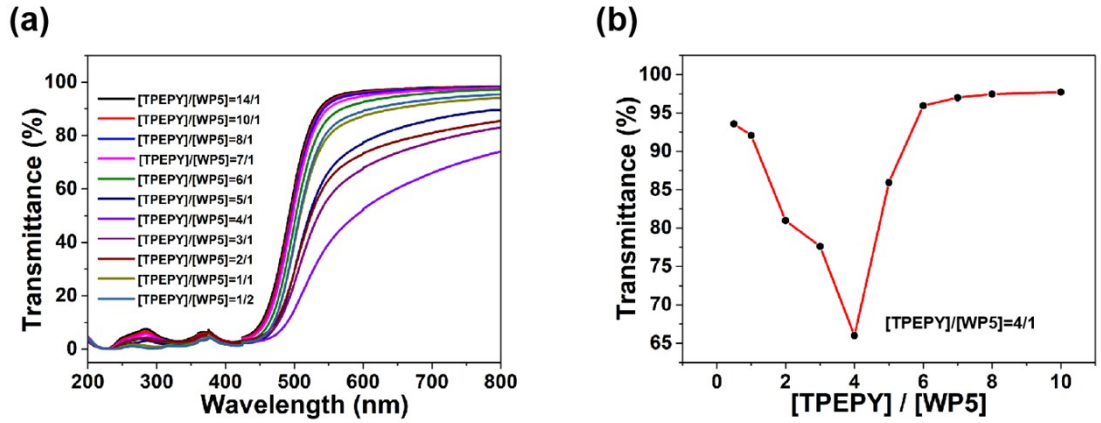

Fig. S16 (a) Optical transmittance of **WP5** and **TPEPY** in water with varied concentrations of **WP5** at a fixed concentration of **TPEPY** (0.05 mM) at 25 °C. (b) Dependence of the relative optical transmittance at 700 nm on **WP5** with a fixed concentration of **TPEPY** (0.05 mM) at 25 °C.

10. Critical aggregation concentration (CAC) investigation of WP5⊃TPEPY nanoassemblies

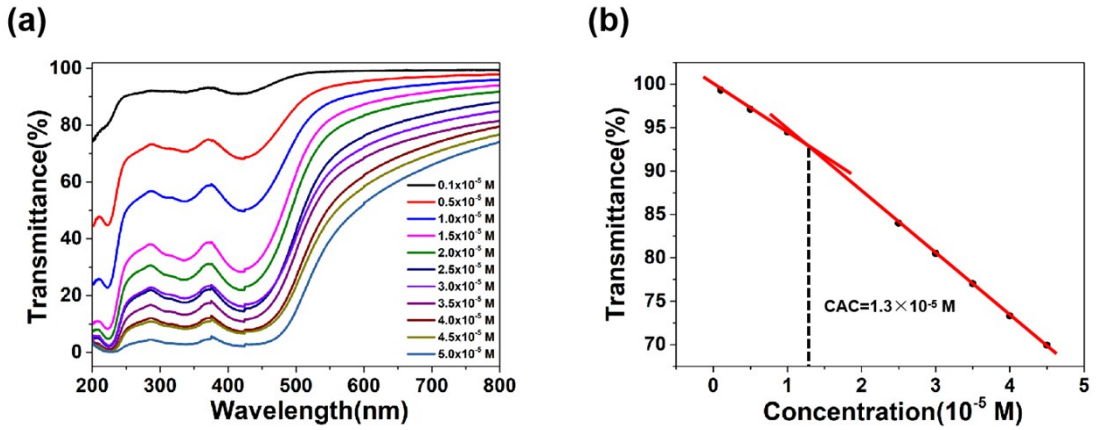

Fig. S17 (a) The concentration-dependent transmittance of **TPEPY** in the presence of **WP5** ([**TPEPY**]/[**WP5**] = 4:1). (b) Dependence of the transmittance of **TPEPY** at 700 nm in the presence of **WP5** ([**TPEPY**]/[**WP5**] = 4:1) under different concentrations.

11. Stability of WP5⊃TPEPY nanoassemblies in water

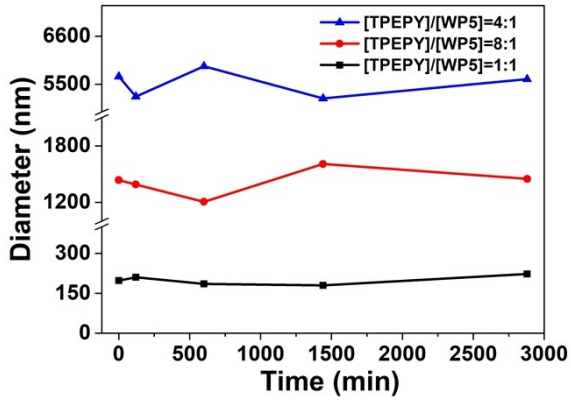

Fig. S18 Time-dependent size changes of **WP5⊃TPEPY** nanoassemblies in water.

12. Absorbance decay of ABDA in the presence of TPEPY and WP5⊃TPEPY nanoassemblies with Fe^{3+} and EDTA

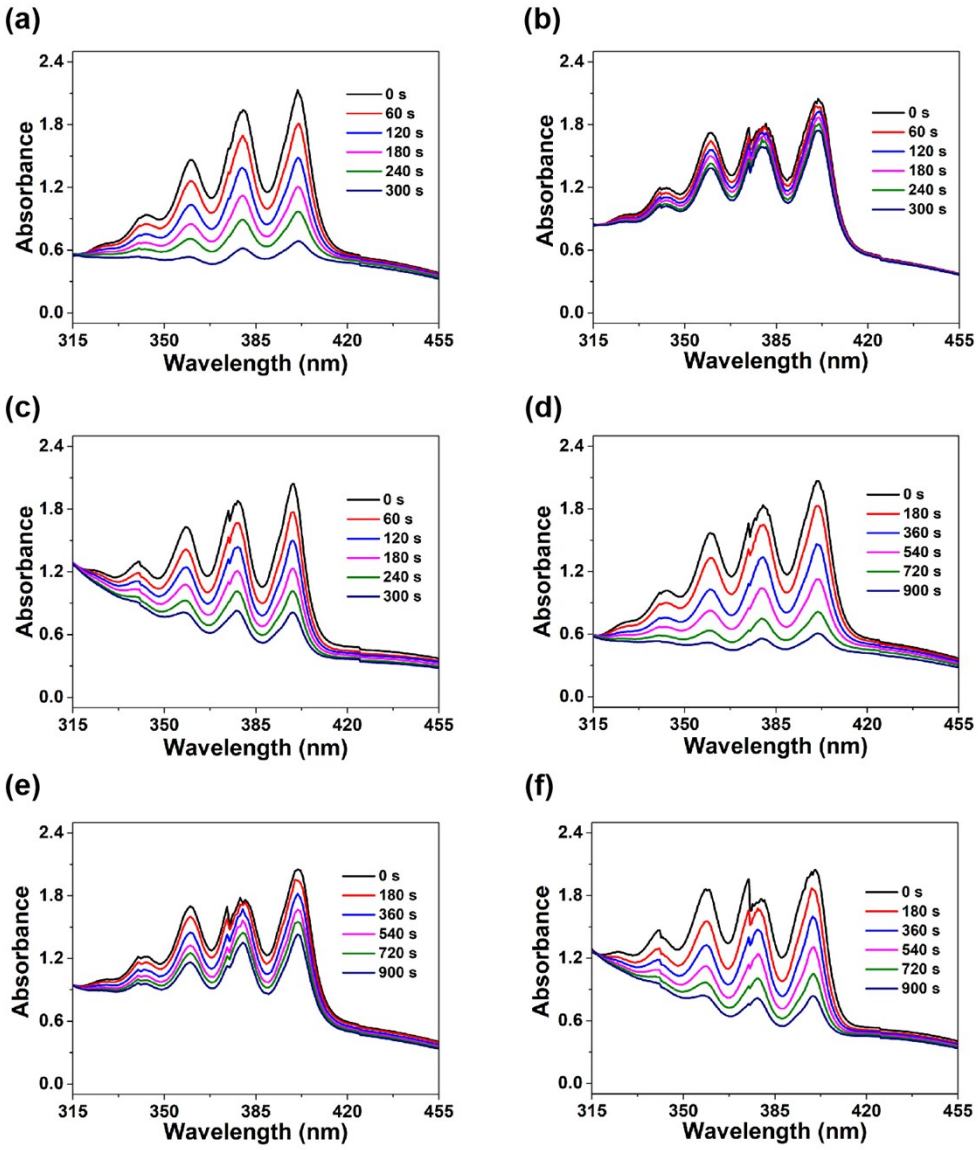

Fig. S19 UV−Vis spectra of ABDA in the presence of **TPEPY** (a), **TPEPY** with Fe^{3+} (b), **TPEPY** with Fe^{3+} and EDTA (c), **WP5⊃TPEPY** (d), **WP5⊃TPEPY** with Fe^{3+} (e), and **WP5⊃TPEPY** with Fe^{3+} and EDTA (f) under white light irradiation (400−700 nm, 10 mW·cm^{-2}). [**TPEPY**] = 15 μM, [**WP5**] = 15 μM, [Fe^{3+}] = 0.18 mM, [EDTA] = 4.50 mM, and [ABDA] = 0.20 mM.

13. Absorbance decay of ABDA in the blank group and in the presence of RB with Fe^{3+}

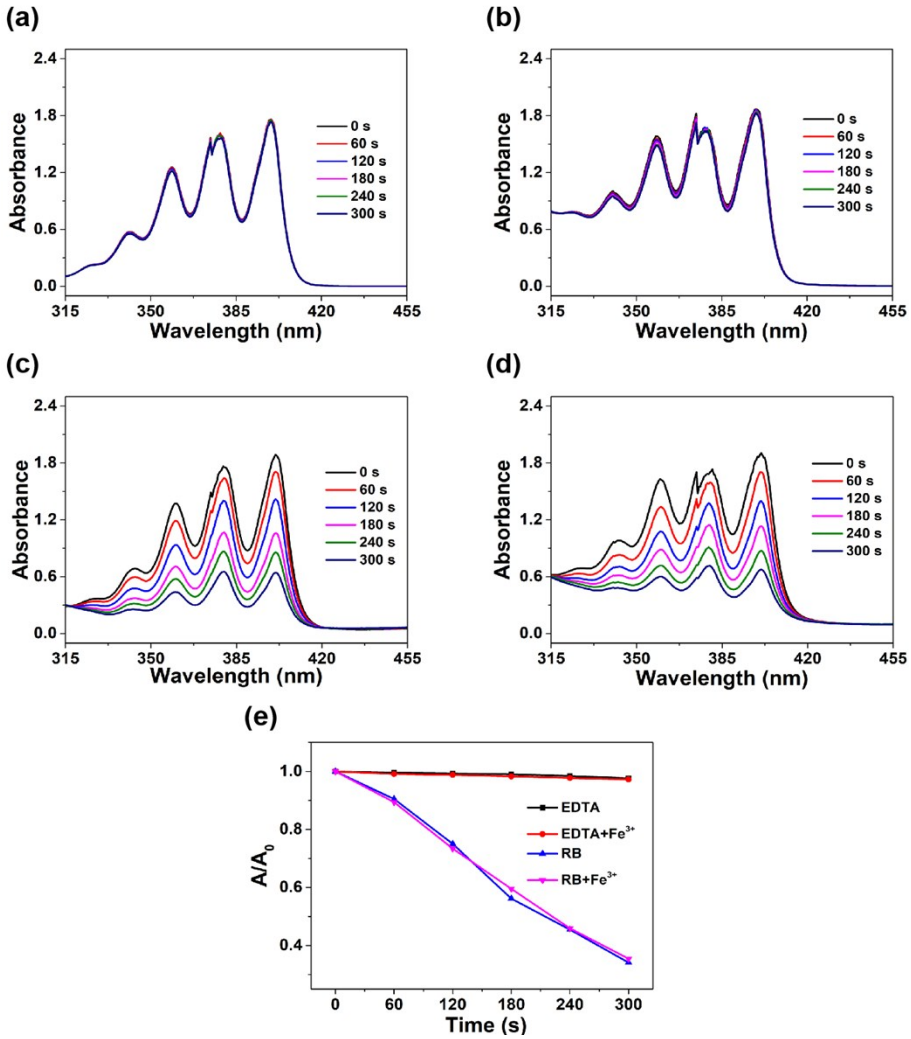

Fig. S20 UV−Vis spectra of ABDA in the presence of EDTA (a), EDTA with Fe^{3+} (b), **RB** (c), and **RB** with Fe^{3+} (d) under white light irradiation (400−700 nm, 10 mW·cm^{-2}). [EDTA] = 4.50 mM, [Fe^{3+}] = 0.18 mM, [**RB**] = 15 μM, and [ABDA] = 0.20 mM.

14. References

S1. M. Zhang, S. Li, X. Yan, Z. Zhou, M. L. Saha, Y. C. Wang and P. J. Stang, *P. Natl. Acad. Sci. USA.*, 2016, **113**, 11100−11105.

S2. Z. Lu, L. He, A. Ding and Z. Tan, CN 106432203, 2017.